

Cluster-void degeneracy breaking: Neutrino properties and dark energy

Martin Sahlén^{1*}

Department of Physics and Astronomy, Uppsala University, SE-751 20 Uppsala, Sweden¹

Future large-scale spectroscopic astronomical surveys, e.g. *Euclid*, will enable the compilation of vast new catalogues of clusters and voids in the galaxy distribution. By combining the constraining power of both cluster and void number counts, such surveys could place stringent simultaneous limits on the sum of neutrino masses M_ν and the dark energy equation of state $w(z) = w_0 + w_a z/(1+z)$. For minimal normal-hierarchy neutrino masses, we forecast that *Euclid* clusters + voids ideally could reach uncertainties $\sigma(M_\nu) \lesssim 15$ meV, $\sigma(w_0) \lesssim 0.02$, $\sigma(w_a) \lesssim 0.07$, independent of other data. Such precision is competitive with expectations for e.g. galaxy clustering and weak lensing in future cosmological surveys, and could reject an inverted neutrino mass hierarchy at $\gtrsim 99\%$ confidence.

I. INTRODUCTION

Galaxy clusters and voids can be used to place constraints on cosmological models. The abundances of clusters and voids are sensitive to dark energy [1–3], modified gravity [1, 4, 5], neutrino properties [6, 7], and non-Gaussianity [8].

The ongoing development of void cosmology is a promising new prospect for large-scale astronomical surveys with unprecedented area, depth and resolution. In a series of papers, we are outlining the potential of void surveys to constrain cosmological models, especially in combination with galaxy cluster surveys. In an earlier work [3], we derived the first cosmological parameter constraints from voids, showing that the joint existence of the largest known cluster and void strongly requires dark energy in the flat Λ CDM model [with cosmological constant Λ and cold dark matter (CDM)]. We also reported a powerful complementarity between clusters and voids in parameter constraints for the Λ CDM model. In subsequent work [5], we investigated the complementarity between cluster and void abundances for constraining deviations from general relativity (GR) on cosmological scales.

Here, we investigate the ability of future *Euclid*-like surveys of clusters and voids to constrain neutrino masses and dark energy properties.

II. MODEL

A. Cosmological model

We assume a flat CDM cosmology, and dark energy with equation of state $w(z) = w_0 + w_a z/(1+z) = w_0 + w_a(1-a)$, the CPL parameterization [9, 10] (where a is the scale factor). In the following, we will consistently use the term “dark matter” to denote all forms of dark matter (including neutrinos), and “cold dark matter” for non-neutrino (cold) dark matter only. The primordial density perturbations are adiabatic and follow a power-law power spectrum. The main

fiducial model is specified by the *Planck* 2015¹ [12] best-fitting flat Λ CDM parameter values: current Hubble parameter $h = 0.673$, current mean matter density $\Omega_m = 0.314$, dark energy equation of state parameters $w_0 = -1$, $w_a = 0$, current mean baryonic matter density $\Omega_b = 0.0492$, current matter power spectrum normalization $\sigma_8 = 0.831$, scalar spectral index $n_s = 0.965$. Neutrinos are modeled with one massive eigenstate and two massless ones, using a sum of neutrino masses $M_\nu = 0.06$ eV (the approximate minimum value allowed by neutrino oscillation data [e.g. 13] and the standard value assumed in many cosmological analyses, e.g. for *Planck* [11, 12]). Hence, the early-universe effective relativistic degrees of freedom $N_{\text{eff}} = 3.046$ [14, 15]. We also investigate the sensitivity of our results to the choice of fiducial model, by also considering an alternative fiducial model for which instead $h = 0.7$, $\Omega_m = 0.3$, $\sigma_8 = 0.8$.

B. Surveys

We examine the *Euclid* Wide Survey [16], covering 15 000 square degrees. For clusters, we consider two cases: the full redshift range $z = 0.2 - 2.0$ (data set EC), and a low-redshift version covering $z = 0.2 - 0.7$ (data set EC-LO). The latter will be used to assess the impact of neglecting cluster-void correlations in the analysis. The lower limit for the cluster mass is $M_{200,c} = 8 \times 10^{13} h^{-1} M_\odot$ (where $M_{200,c}$ is the halo mass within a volume defined by an overdensity threshold of 200 above the critical density). A constant 80% completeness is assumed [17]. We use bins in redshift $\Delta z = 0.1$ and in cluster mass $\Delta \log(M_{200}) = 0.2$.

For voids, we limit the analysis to spectroscopic data, $z = 0.7 - 2.0$, to minimize the impact of redshift-space systematics. Void selection is assumed complete above the limiting radius $R_{\text{lim}}(z) = 2\bar{n}_{\text{gal}}^{-1/3}(z)$ [2], where $\bar{n}_{\text{gal}}(z)$ is the mean comoving galaxy number density. See [5] for de-

*Electronic address: msahlen@msahlen.net

¹ The preprint of the *Planck* 2018 results [11] appeared after submission of this work. We focus on the 2015 best-fit cosmology for direct comparability to other forecasts in the literature, but discuss the impact of an alternative fiducial cosmology, with predicted number counts almost identical to those for the *Planck* 2018 results (see main text).

tails. We model the *Euclid* galaxy bias as [18]

$$b_g(z) = \sqrt{1+z}. \quad (1)$$

We note that the galaxy bias in reality depends on the neutrino mass in a scale-dependent manner. The effect on the galaxy bias of an increase in the neutrino mass is a constant enhancement of small-scale bias, and a scale-dependent, increasing bias towards large scales ($k \lesssim 0.1 h \text{ Mpc}^{-1}$). For the values of neutrino masses we consider, this effect is of the order a few percent [e.g. 19–21], and we ignore it in our analysis. However, for sufficiently large neutrino masses, and voids defined by highly biased tracers, this effect on the tracer bias can even reverse the pattern of enhancement and suppression of abundances seen in the dark matter field as neutrino mass increases [21].

For *Euclid* voids we consider two binning schemes:

EV-A Bins in redshift $\Delta z = 0.1$ and one bin in radius $R > R_{\text{lim}}(z)$ and void galaxy field density contrast $\delta_g^v < -0.8$.

EV-B Bins in redshift $\Delta z = 0.1$, in void radius $\Delta \log(R) = 0.1$, and three bins in void galaxy field density contrast in the range $-1 < \delta_g^v < -0.25$, with $\Delta \delta_g^v = 0.25$ (corresponding to deep, medium and shallow voids).

These binnings should accommodate expected measurement uncertainties. The two binning cases can be regarded as worst-case and best-case scenarios with respect to the capability to successfully model and observationally extract void abundances from galaxy surveys.

C. Cluster and void abundance with neutrinos

We predict cluster and void abundances adopting models and methodology developed in earlier work [3, 5, 22]. As in [5], we include scatter in cluster mass and void radius determinations, and also vary the characteristic void density contrast (through the parameter D_v , see below). We neglect cluster-void correlations, but make conservative overestimates of their impact on the results, by considering the low-redshift cluster survey EC-LO which has no overlapping volume with the void surveys.

In comparison to massless neutrinos, massive neutrinos effectively shift the turnover scale in the matter power spectrum, and suppress power below the neutrino free-streaming scale. This tends to delay and suppress the formation of clusters and voids. In our fiducial dark energy model, the neutrino free-streaming scale is given by [e.g. 23]

$$k_{\text{FS}}^\nu(z) \approx 0.8 \frac{\sqrt{0.686 + 0.314(1+z)^3}}{(1+z)^2} \left(\frac{M_\nu}{1 \text{ eV}} \right) h \text{ Mpc}^{-1}. \quad (2)$$

Additionally, the linear growth rate of over- and underdensities is slightly reduced since free-streaming neutrinos lack gravitational backreaction.

The local neutrino density will also influence the non-linear evolution of clusters and voids. We describe below the modeling of the effects of neutrinos on non-linear structure formation based on good first-order approximations.

1. Cluster abundance

For galaxy clusters, the effect of neutrinos is modeled following Brandbyge et al. [6]. On cluster scales, neutrinos free-stream and do not participate in gravitational collapse. Cluster masses are accordingly rescaled: $M = 4\pi R_L^3 [(1 - f_\nu)\rho_m + f_\nu\rho_b]/3$, where R_L is the Lagrangian radius corresponding to the cluster, ρ_m is the mean matter density, $f_\nu = [M_\nu/93 \text{ eV}]/\Omega_{\text{dm}} h^2$ is the fraction of the dark matter density Ω_{dm} in neutrinos, and ρ_b is the mean baryon density.

2. Void abundance

For voids, we model the effect of neutrinos by extending the treatment in [3]. When neutrinos have nonzero mass, the neutrino density contributes to the dynamical evolution of a void, but does not have a significant density contrast on its own, except for voids larger than the neutrino free-streaming length [e.g. 7, 19, 20]. If an effective fraction $f_{\text{cl}}(R, z; f_\nu)$ of matter participates in clustering below the co-moving scale R at redshift z , the total void matter density contrast will be

$$\delta_m^v = f_{\text{cl}}(R, z; f_\nu) \delta_{\text{cdm}}^v, \quad (3)$$

where δ_{cdm}^v is the non-neutrino cold dark matter density contrast of the void. We can write the clustering fraction as

$$f_{\text{cl}}(R, z; f_\nu) = 1 - f_{\text{dm}} f_\nu f_{\text{FS}}(R, z; f_\nu). \quad (4)$$

Here $f_{\text{dm}} = 1 - \Omega_b/\Omega_m$ (The earlier work [3] contained a typographical sign error in Sec. 3.1.5.) is the fraction of matter in dark matter (including neutrinos), and

$$f_{\text{FS}}(R, z; f_\nu) \approx 1 - e^{-R_{\text{FS}}^\nu(z)/R} \quad (5)$$

is the effective fraction of neutrinos that do not participate in clustering due to free-streaming below the neutrino free-streaming length $R_{\text{FS}}^\nu = 2\pi/k_{\text{FS}}^\nu$. Since galaxies trace the cold dark matter field, we assume that

$$\delta_{\text{cdm}}^v = b_g^{-1}(z) \delta_g^v, \quad (6)$$

where b_g is the bias relative to the density contrast δ_g^v in the galaxy field of the survey.

We model the evolution of individual voids using the spherical expansion model, whereby the under-density evolves as a separate universe embedded in the background [20, 24, 25]. When the fraction of dark matter in neutrinos is small, $0 < f_\nu \ll 1$, voids evolve approximately as in a $f_\nu = 0$ cosmology but rescaled by f_{cl} : the nonlinear matter density contrast δ_m^v of a void is well approximated by

$$\delta_m^v = f_{\text{cl}}^{-1}(R, z; f_\nu) \delta_m^{v,0}, \quad (7)$$

where $\delta_m^{v,0}$ is the spherical-expansion solution for $f_\nu = 0$. The relation between non-linear and linear void radii is given by

$$\frac{R}{R_L} = (1 + \delta_m^{v,0})^{-1/3} = (1 + f_{cl}(R, z; f_\nu) \delta_{cdm}^{v,0})^{-1/3}. \quad (8)$$

The relationship between linear and nonlinear density contrast when $f_\nu = 0$ is well approximated by [25, 26]

$$\delta_{lin,m}^{v,0}(\delta_m^{v,0}) = c \left[1 - (1 + \delta_m^{v,0})^{-1/c} \right], \quad (9)$$

with $c = 1.594$ (we take the same approach as e.g. [27]). Hence, for $0 < f_\nu \ll 1$, the relationship between linear and nonlinear density contrast is given by

$$\delta_{lin,m}^v(R, z) = f_{cl}^{-1}(R, z; f_\nu) \delta_{lin,m}^{v,0}(\delta_m^{v,0}) \quad (10)$$

$$= f_{cl}^{-1}(R, z; f_\nu) \times \delta_{lin,m}^{v,0}(f_{cl}(R, z; f_\nu) \delta_m^v) \quad (11)$$

$$= f_{cl}^{-1}(R, z; f_\nu) \times \delta_{lin,m}^{v,0}(f_{cl}^2(R, z; f_\nu) \delta_{cdm}^v). \quad (12)$$

In practice, the corrections to the spherical-expansion dynamics compared to $f_\nu = 0$ are $\sim 1-2\%$ for values of the neutrino mass $M_\nu < 0.15$ eV.

We employ the volume-conserving ‘‘VdN’’ void abundance model [25], with the ‘‘1LDB’’ multiplicity function (MF) [28]

$$f(\sigma) = \frac{|\delta_{lin,m}^v|}{\sigma \sqrt{1 + D_v}} \sqrt{\frac{2}{\pi}} \exp \left[-\frac{(|\delta_{lin,m}^v| + \beta_v \sigma^2)^2}{2\sigma^2(1 + D_v)} \right], \quad (13)$$

where $\delta_{lin,m}^v$ is given by Eqs. (12) and (6). The matter-field dispersion $\sigma(R_L, z)$ is calculated on the scale R_L given by Eq. (8), at redshift z . Based on the findings of [29], we set the constant $\beta_v = 0$ for simplicity. Note that we vary D_v alongside the cosmological parameters in our analysis to account for theoretical uncertainty in the void abundance model. To match the N -body results for *Euclid*-like surveys in [2], we first normalize the void number density by the relative VdN volume factor

$$\left[\frac{V(R_L)}{V(R)} \right]_{\text{Pisani}}^{-1}, \quad (14)$$

appropriate for those simulations, where $V(R) = 4\pi R^3/3$ is the void volume. We set the fiducial value of $D_v = 3.38$. This prescription matches the void abundance results in [2] and [29], taking the relevant cosmological parameters and survey galaxy bias into account. In [2] it is found that D_v can be assumed independent of redshift within uncertainties, and [29] finds that a single value of D_v is valid for different δ_g^v as long as the galaxy bias b_g is taken into account according to Eq. (6) when computing $\delta_{lin,m}^v$. This is expected since the matter-field dispersion $\sigma(R_L) \sim R_L^{-\gamma(R_L)}$, where $\gamma(R_L)$ is only weakly dependent on R_L [30]. A relative difference in radius between the galaxy and dark matter fields therefore approximately corresponds to rescaling σ by a constant, which is what $\sqrt{1 + D_v}$ effectively does.

III. METHOD

We compute expected parameter constraints using the Fisher matrix method, based on the Poissonian number counts [5]. The space of nine free parameters is defined by $\{\Omega_m, M_\nu, w_0, w_a, \sigma_8, n_s, h, \Omega_b, D_v\}$. We also consider the eight-parameter constant equation of state case, where $w_a = 0$. Cosmological quantities are computed with a modified version of CAMB [9].

We compute forecast Bayes factors for a normal neutrino hierarchy vs. an inverted hierarchy, assuming the normal-hierarchy fiducial model. From this we can estimate the significance with which a minimal normal hierarchy can be distinguished from an inverted hierarchy in the model inference sense, with the different surveys considered.

The posterior odds for normal hierarchy vs. inverted hierarchy is given by [31–34]

$$\frac{p(\text{NO}|d)}{p(\text{IO}|d)} = B_{\text{NO,IO}} \frac{\pi(\text{NO})}{\pi(\text{IO})}, \quad (15)$$

where ‘‘NO’’ denotes normal ordering, ‘‘IO’’ denotes inverted ordering, d is the data under consideration, $B_{\text{NO,IO}}$ is the Bayes factor (see below), and π denotes the prior model probabilities. We assume here that $\pi(\text{NO}) = \pi(\text{IO})$, and therefore the posterior odds are given by $B_{\text{NO,IO}}$. The Bayes factor $B_{\text{NO,IO}}$ is the Bayesian evidence ratio:

$$B_{\text{NO,IO}} = \frac{\int_{M_{\text{IO}}^{\min}}^{\infty} \int_{\theta} \mathcal{L}(d|\theta, M_\nu; \text{NO}) \pi(\theta) \pi(M_\nu) d\theta dM_\nu}{\int_{M_{\text{NO}}^{\min}}^{\infty} \int_{\theta} \mathcal{L}(d|\theta, M_\nu; \text{IO}) \pi(\theta) \pi(M_\nu) d\theta dM_\nu}, \quad (16)$$

where $\mathcal{L}(d|\theta, M_\nu; H)$ is the likelihood function for the data d given model parameters θ and M_ν under the neutrino hierarchy hypothesis H . The priors $\pi(\theta)$ and $\pi(M_\nu)$ are chosen as flat (uniform) in all parameters and nonrestrictive with respect to the likelihood function.

We set $M_{\text{NO}}^{\min} = 0.06$ eV, $M_{\text{IO}}^{\min} = 0.10$ eV [35]. The confidence level of the rejection of the disfavoured model (in this case the inverted neutrino hierarchy, since we are assuming a minimal normal neutrino hierarchy) is

$$1 - \alpha = 1 - |B_{\text{NO,IO}}|^{-1} \quad (17)$$

which can also be translated to an effective ‘‘number of σ ’’ confidence level n_σ^{eff} defined by the equation

$$\text{erf} \left(\frac{n_\sigma^{\text{eff}}}{\sqrt{2}} \right) = 1 - \alpha. \quad (18)$$

Dark energy Figures of Merit are computed as

$$\text{FoM}(w_0, w_a) = \frac{1}{\sqrt{\det \text{cov}(w_0, w_a)}}. \quad (19)$$

IV. RESULTS

A. Forecast parameter constraints

The marginalized constraints from *Euclid* on the summed neutrino mass M_ν are shown in Fig. 1, while the results for all

TABLE I: Forecast 68% parameter uncertainties (unless otherwise specified), significance levels of neutrino-hierarchy model inference, and dark energy Figures of Merit from cluster and void abundances in future *Euclid*-like surveys. See Secs. II and III for definitions and details.

Data set	Parameter Inference								Neutrino Mass Ordering			DE
	$\sigma(\Omega_{\rm m})$	$\sigma(M_\nu) / \text{CL}$	$\sigma(w_0)$	$\sigma(w_a)$	$\sigma(\sigma_8)$	$\sigma(n_s)$	$\sigma(h)$	$\sigma(\Omega_{\rm b}) / \text{CL}$	$\ln(B_{\rm NO,IO})$	Odds $B_{\rm NO,IO}$	$n_\sigma^{\rm eff}$	FoM
	$w(z) = w_0$											
EV-A	0.04	$< 0.4 \text{ eV (95\%)}$	0.26	–	1.7	0.82	0.05	$\leq \Omega_{\rm m}$	0.3	1.3 : 1	0.27	–
EV-B	0.004	15 meV	0.009	–	0.11	0.02	0.008	0.005	4.9	130 : 1	2.7	–
EC	0.002	$< 1.6 \text{ eV (95\%)}$	0.007	–	0.01	0.08	0.03	$< 0.13 \text{ (95\%)}$	0.0	1.0 : 1	0.05	–
EV-A+EC	0.0006	$< 0.18 \text{ eV (95\%)}$	0.003	–	0.001	0.04	0.02	0.02	1.0	2.8 : 1	0.91	–
EV-A+EC-LO	0.0008	$< 0.18 \text{ eV (95\%)}$	0.01	–	0.005	0.09	0.02	0.03	0.9	2.5 : 1	0.85	–
EV-B+EC	0.0005	10 meV	0.003	–	0.0006	0.01	0.007	0.003	9.7	$1.6 \times 10^4 : 1$	3.5	–
EV-B+EC-LO	0.0007	11 meV	0.003	–	0.002	0.01	0.007	0.003	8.2	$3.6 \times 10^3 : 1$	3.4	–
	$w(z) = w_0 + w_a z / (1 + z)$											
EV-A	0.04	$< 0.8 \text{ eV (95\%)}$	1.1	4.0	1.8	1.1	0.08	$\leq \Omega_{\rm m}$	0.1	1.1 : 1	0.11	1
EV-B	0.004	17 meV	0.03	0.15	0.11	0.02	0.009	0.005	4.0	54 : 1	2.4	750
EC	0.003	$< 1.7 \text{ eV (95\%)}$	0.01	0.04	0.01	0.08	0.03	$< 0.14 \text{ (95\%)}$	0.0	1.0 : 1	0.05	3500
EV-A+EC	0.001	$< 0.18 \text{ eV (95\%)}$	0.01	0.04	0.002	0.04	0.02	0.02	1.0	2.7 : 1	0.89	7500
EV-A+EC-LO	0.003	$< 0.19 \text{ eV (95\%)}$	0.03	0.12	0.006	0.10	0.03	0.03	0.8	2.3 : 1	0.77	640
EV-B+EC	0.001	11 meV	0.009	0.03	0.001	0.01	0.007	0.004	8.2	$3.6 \times 10^3 : 1$	3.4	12000
EV-B+EC-LO	0.002	15 meV	0.02	0.07	0.003	0.02	0.008	0.004	4.9	130 : 1	2.7	4600

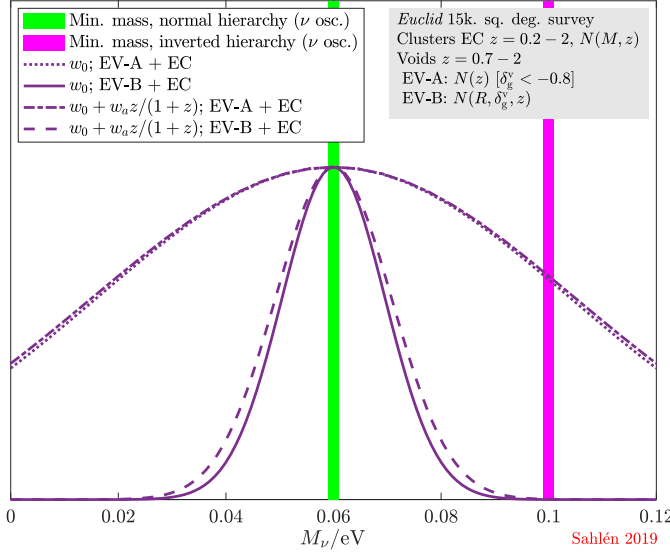


FIG. 1: Forecast marginalized probability density functions (pdfs) for the summed neutrino mass M_ν from cluster and void abundances in the *Euclid* survey. A constant (w_0) or time-varying (w_0, w_a) dark energy equation of state is assumed. See Secs. II and III for definitions and details.

the cosmological parameters are reported in Table I. Figure 2 shows the full set of one-dimensional and two-dimensional marginalized parameter constraints for cluster and void counts in the (w_0, w_a) dark energy model, for EV-B and EC. We omit the results on the nuisance parameter D_v for brevity. Notably, we see in Fig. 2 that cluster and void constraints are orthogo-

nal among many of the model parameters. Clusters are most sensitive to dark energy parameters, and voids most sensitive to the sum of neutrino masses. The combination of deep and shallow void counts (in EV-B) can powerfully break degeneracies between background expansion, shape of the power spectrum, and growth history [5], akin to a multi-tracer approach. Clusters of galaxies have complementary sensitivity to expansion history, growth history and power spectrum scales, so that combining cluster and void counts further breaks degeneracies [3, 5]. In terms of structure growth, a void survey at redshift z can be regarded as roughly equivalent to a cluster survey at redshift $z + 0.5$ (since the nonlinear collapse / shell-crossing thresholds are $\delta_{\text{nl}}^{\text{cluster}} \sim 1.7$, $\delta_{\text{nl}}^{\text{void}} \sim -2.7$ in terms of extrapolated linear density), but with orthogonal degeneracy between Ω_m and σ_8 . These features explain the ability of void counts to constrain all parameters in our model, the strengthening of constraints when cluster counts are added, and the fact that many parameter constraints remain nearly unchanged when an additional parameter (w_a) is considered.

We see from Table I that if voids binned in void radius and density contrast (EV-B) are combined with clusters (EC), we expect to measure the summed neutrino mass with an uncertainty $\sigma(M_\nu) \lesssim 15 \text{ meV}$. When the total abundances of deep voids above the limiting radius in redshift bins (EV-A) are combined with clusters (EC), we expect only marginally competitive constraints of $M_\nu \lesssim 0.19 \text{ eV (95\% CL)}$. Still, the combined constraints are significantly tighter than for the individual cluster and void surveys, and provide an independent test based on large-scale structure only. These results do not change when a constant (one-parameter) or time-dependent (two-parameter) dark energy equation of state is assumed (see Fig. 1).

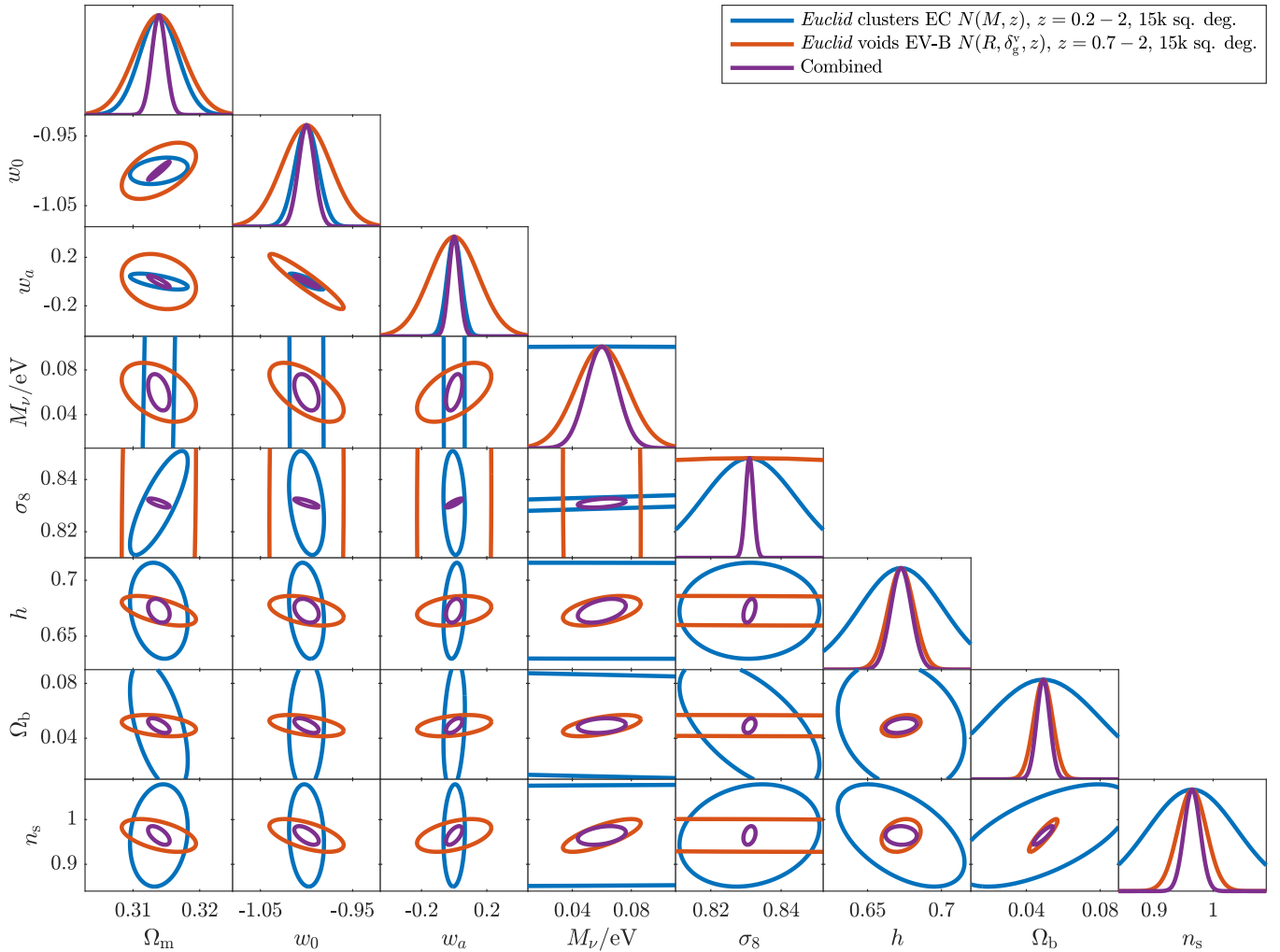


FIG. 2: Forecast 68% parameter contours, and marginal probability density functions, from cluster and void abundances in future *Euclid* surveys. A dark energy equation of state $w(z) = w_0 + w_a z/(1+z)$ is assumed. See Secs. II and III for definitions and details.

For the dark energy equation of state with EV-B + EC, we forecast combined cluster-void constraints $\sigma(w_0) \lesssim 0.02$, $\sigma(w_a) \lesssim 0.07$, $\text{FoM}(w_0, w_a) \gtrsim 4600$. In the worst-case scenario EV-A + EC, the combined cluster-void constraints do not improve on the cluster-only (EC) constraints $\sigma(w_0) \lesssim 0.01$, $\sigma(w_a) \lesssim 0.04$, $\text{FoM}(w_0, w_a) \gtrsim 3500$.

For simplicity, we have neglected spatial cluster-void correlations. We may therefore be overestimating the statistical power of our joint cluster-void analysis. To investigate the possible degradation of parameter constraints due to cluster-void correlations, we consider the alternative cluster survey EC-LO truncated at $z = 0.7$ (the lower redshift limit of the void survey). Thus, we throw away the clusters in the EV-A/B + EC overlapping volume across $z = 0.7 - 2.0$. The uncertainties on M_ν are robust to within 10% in this analysis. The uncertainties on w_0 and w_a increase by a factor of a few, but we note that the full cluster-only parameter uncertainties (EC) are significantly smaller in comparison.

To demonstrate that the results are stable against changes

in fiducial cosmology, we repeated the analysis using an alternative fiducial model, with differing values $h = 0.7$, $\Omega_m = 0.3$, $\sigma_8 = 0.8$. We have confirmed that the predicted number counts for this model are identical with those for the *Planck* 2018 best-fit model [11], to within a few per cent. For these two models, the parameter uncertainties are marginally larger for the different individual and joint cases, but within rounding error. The only exception is the case where we consider EV-A data only, for which parameter uncertainties are a factor 2–4 larger (except for $\sigma(\sigma_8)$, which is unchanged).

B. Void parameter sensitivity

The sensitivity of void counts to changes in the parameters w_0 , w_a and M_ν is shown in Fig. 3 (see also Fig. 3 of Ref. [5]).

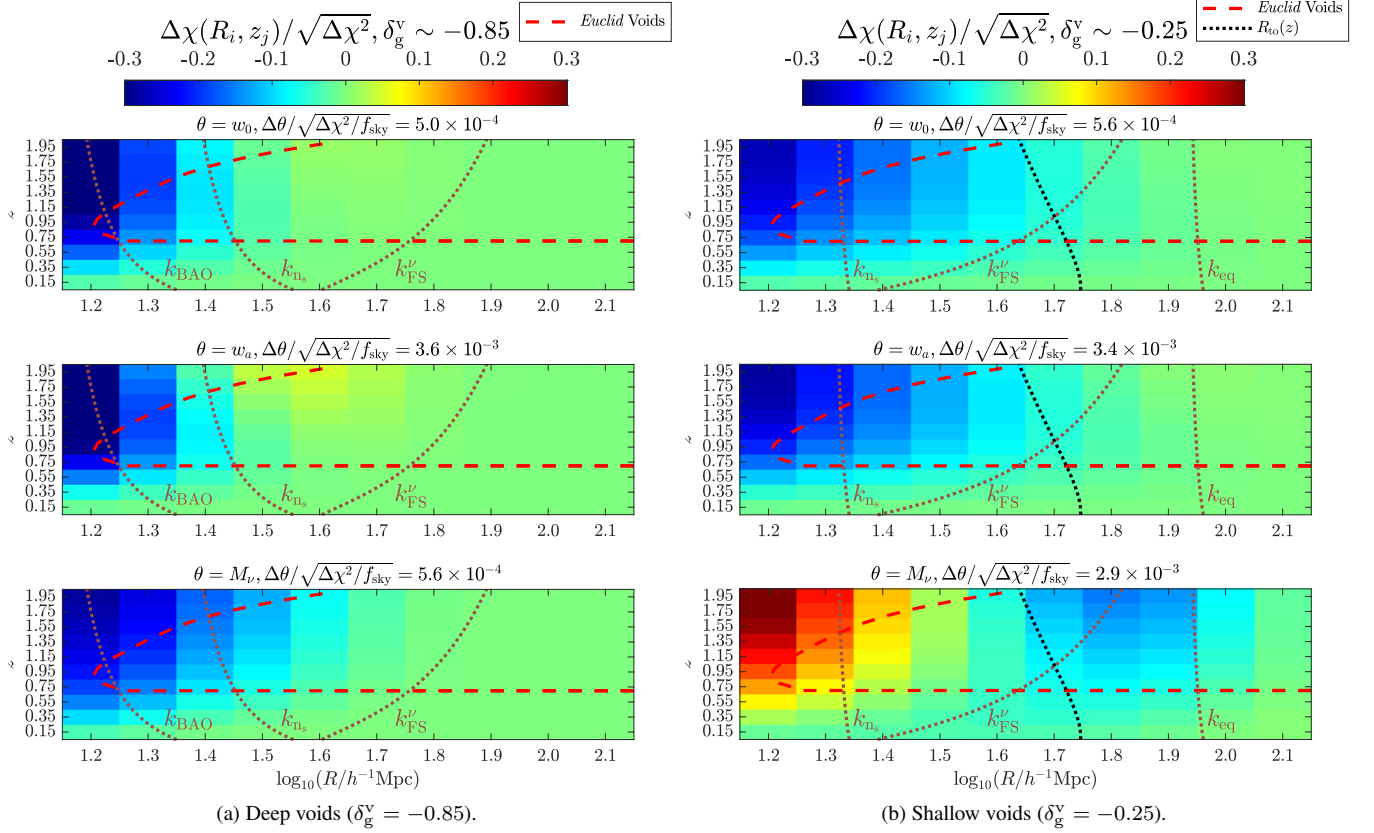


FIG. 3: Void parameter sensitivity. We here use a generic void survey with $R_{\text{lim}} = 14 h^{-1} \text{Mpc}$ and $z = 0.05 - 2.05$, $\Delta \log_{10}(R/h^{-1} \text{Mpc}) = 0.1$, $\Delta z = 0.2$. For each parameter, the figure shows $\Delta \chi_{i,j}^{\text{rel}}$ when that parameter *only* is varied. Hence, σ_8 is kept normalized to the fiducial value when other parameters are varied. See [5] for additional parameters. The turnover radius $R_{\text{to}}(z)$ is shown in black, dotted lines. Scales related to the cosmological parameters are shown in brown, dotted lines ($k_{\text{BAO}} = 0.06 h \text{Mpc}^{-1}$, $k_{\text{ns}} = 0.05 h \text{Mpc}^{-1}$, $k_{\text{FS}}^{\nu} \sim 0.003 - 0.05 h \text{Mpc}^{-1}$, $k_{\text{eq}} = 0.012 h \text{Mpc}^{-1}$). The coverage of the *Euclid* void surveys in terms of limiting radii and redshift is shown in red, dashed lines. See Sec. IV B for definitions and details.

We illustrate sensitivity using the quantity

$$\Delta \chi_{i,j}^{\text{rel}}(\Delta \theta_k) \equiv \frac{\Delta \chi(R_i, z_j; \Delta \theta_k, f_{\text{sky}})}{\sqrt{\Delta \chi^2(\Delta \theta_k, f_{\text{sky}})}}, \quad (20)$$

for a small positive one-parameter shift $\Delta \theta_k$ away from the fiducial cosmological model. Here, the quantity $\Delta \chi$ represents the number count change in bin i, j , in units of Poisson uncertainty, under the shift $\Delta \theta_k$:

$$\Delta \chi(R_i, z_j; \Delta \theta_k, f_{\text{sky}}) = \sqrt{\frac{2 f_{\text{sky}}}{N_{i,j}}} \frac{\partial \bar{N}_{i,j}}{\partial \theta_k} \Delta \theta_k. \quad (21)$$

The quantity $\Delta \chi^2$ is the total change in χ^2 across all bins under the shift $\Delta \theta_k$:

$$\Delta \chi^2(\Delta \theta_k, f_{\text{sky}}) = \sum_{i,j} \Delta \chi^2(R_i, z_j; \Delta \theta_k, f_{\text{sky}}). \quad (22)$$

Above, bins in radius and redshift are indexed by i and j , $\bar{N}_{i,j}$ is the fiducial expected number of voids in bin (i, j) , and f_{sky} is the survey fractional sky coverage. Note that $\Delta \chi_{i,j}^{\text{rel}}$

is independent of the survey sky fraction f_{sky} , and represents the statistical significance of the number count change in bin i, j relative to average statistical significance of number count changes in all bins, under the shift $\Delta \theta_k$ [5].

Figure 3 also shows the void turnover scale $R_{\text{to}}(z)$ (right panel only, as it is below the limiting radius in the left panel), here defined by

$$\nu(R_{\text{to}}, z) = 1, \quad (23)$$

where

$$\nu(R, z) = \frac{|\delta_{\text{lin},m}^{\nu}(R, z)|^2}{\sigma^2(R, z)(1 + D_{\nu})}, \quad (24)$$

assuming $\beta_{\nu} = 0$ in Eq. (13). Above the turnover radius, the sensitivity to the matter power spectrum and growth history gradually dominates over the sensitivity to the expansion history [5]. Note that the linear-density threshold $\delta_{\text{lin},m}^{\nu}$ is redshift-dependent, as the survey galaxy bias.

The top two panels in Fig. 3 show that when the dark energy equation of state (w_0 or w_a) is increased, the effect on void

abundances is simple for both deep ($\delta_g^v \sim -0.85$) and shallow ($\delta_g^v \sim -0.25$) voids: the cosmic volume is reduced, and hence the void abundance suppressed. For sufficiently rare voids, however, the relatively enhanced growth overtakes the volume suppression to enhance the void abundance. The impact of variations in the dark energy equation of state and the linear growth rate is discussed in more detail in [5].

When the neutrino mass M_ν is varied, the effect is significantly different for deep and shallow voids, as seen in the bottom panels of Fig. 3. Thus, the balance of the abundances of small and large voids of different depth should be a good probe of neutrino mass. A key to this effect is the location of the turnover radius, which implies that the effect is the result of an interplay between $\sigma(R, z)$, $b_g(z)$, $f_{cl}(R, z)$ and D_v (in addition to the dependence on δ_g^v). Hence, the two distinct effects can also be replicated by considering tracers with low and high bias, respectively.

In the following, we describe the impact on void abundances from changing the total neutrino mass, as demonstrated in Fig. 3. If M_ν is increased, the matter power spectrum is significantly suppressed below the free-streaming scale k_{FS}^ν . The suppression tapers out towards $k_{eq} \sim 0.01 h \text{ Mpc}^{-1}$. In Fig. 3 we keep the matter power spectrum normalized to the fiducial value of σ_8 (at $z = 0$) when increasing M_ν . Hence, the overall effect is to suppress the matter power spectrum for $k \gtrsim k_{eq}$ and enhance it for $k \lesssim k_{eq}$; the relative difference increasing with redshift.

The value of $\sigma(R, z)$, the matter power spectrum at redshift z averaged on the scale R , is suppressed or enhanced with the power spectrum itself. Since

$$\frac{d \ln f}{d \ln \sigma} = \nu - 1, \quad (25)$$

for $\beta_v = 0$ in Eq. (13), void abundances are increased or reduced according to their fiducial value of ν when σ changes. The turnover radius $R_{to}(z)$ marks the transition between increase and reduction. A negative shift $-\Delta\sigma$, due to e.g. increased neutrino suppression, produces a reduction of small/common voids ($\nu < 1$) and an increase of large/rare voids ($\nu > 1$). Note that the value of ν depends on the galaxy bias b_g through $\delta_{lin,m}^v$.

The most significant effect on deep voids is straightforward. These voids are all larger than the turnover radius, and the suppression of the power spectrum increases the values of ν for the voids. Therefore, by Eq. (25), the void abundances are reduced.

The most significant effects on shallow voids are complicated by the fact that the turnover radius lies within the survey. This is because shallow voids are close to linear with almost equal Eulerian and Lagrangian radii. Some smaller voids here lie below the turnover radius, and have $\nu < 1$. The abundance of such voids is increased when the power spectrum is suppressed, by Eq. (25). Above the turnover radius, however, the abundance of larger voids is instead reduced as a consequence of the power-spectrum suppression (as for deep voids). On large scales, $k \lesssim k_{eq}$, the effective enhancement of the matter power spectrum (due to keeping σ_8 fixed, as discussed above) means that the abundance of the largest voids is instead in-

creased.

C. Forecast neutrino hierarchy constraints

In Table I, we report forecast values for the Bayes factor (odds) $B_{NO,IO}$, its logarithm $\ln(B_{NO,IO})$, and the effective significance level n_σ^{eff} with which the inverted hierarchy can be rejected (all under the assumption of a fiducial minimal normal neutrino hierarchy). The EC cluster survey and EV-A void survey cannot distinguish between the two different neutrino hierarchies on their own. The EV-B void survey and the combined EV-B + EC surveys could provide strong or decisive evidence against the inverted hierarchy, while the combined EV-A + EC surveys would only provide weak evidence against the inverted hierarchy (in the language of the conventional Jeffreys scale [36]).

Like for the forecast parameter constraints, we also make a very conservative estimate of the potential degradation of our results due to cluster-void correlations, by completely throwing away the clusters in the overlapping volume across $z = 0.7 - 2.0$ (EC-LO). We find that the above conclusions are robust with respect to cluster-void correlations.

For the alternative fiducial model, in which we set $h = 0.7$, $\Omega_m = 0.3$, $\sigma_8 = 0.8$, the evidence against the inverted neutrino hierarchy is only marginally weaker than for the *Planck* 2015 cosmology. Conclusions remain unchanged.

D. Systematics

The void abundance model is approximate, and a phenomenological extension of fits to N -body simulations. To account for observational and theoretical uncertainty, we include statistical scatter in void radius measurements (and likewise for cluster mass) and allow the characteristic void density contrast to vary through the parameter D_v in the analysis. We see no significant difference in the constraints compared to keeping the value of D_v fixed. This is in line with earlier findings [2]. Also, recent studies indicate that the tracer bias remains simple within voids [37, 38]. This suggests that bias-weighted modeling of void abundances of different depth as used here can be expected to work fairly well. Nevertheless, the relation between galaxy bias of voids and the large-scale galaxy bias of a survey is in general scale/density-dependent. Neutrinos also induce a weak scale dependence in the bias [19, 20]. We expect that the impact of these features is relatively small and within the uncertainty included on D_v , but these aspects (and the impact of full halo occupation statistics) require further simulation studies and method development. A promising approach is the “cleaning method” of Ronconi and Marulli [27]. Void selection and other potential sources of observational bias also require more detailed studies.

We neglect the impact of cluster-void correlations in our main analysis, but find that even when discarding all clusters in the overlapping volume between *Euclid* clusters and voids (EC-LO), the combined cluster + void neutrino-mass

constraints are degraded only marginally. Dark energy constraints are degraded by at most a factor of a few (though in an exact treatment presumably less, since the full cluster-only constraints EC are significantly tighter).

There is additional cosmological information in void samples that we have not considered here. We have limited the analysis to $z = 0.7 - 2$ for *Euclid*, for which spectroscopy is expected and hence redshift-space systematics should be minimal. The sample could be extended down to $z = 0.2$ using photometry. The ellipticity distribution of voids is sensitive to cosmological parameters (including neutrino mass) [7]. The shapes and dynamics of voids are also independently sensitive to the expansion history and growth rate [39], providing further prospects for limiting the effects of systematics. The combination of deep + medium + shallow void counts should further help calibrate void systematics [5].

We argue therefore that the EV-A and EV-B cases can be regarded as worst-case and best-case scenarios for voids. The cluster constraints can be considered a best-case scenario, though imperfect knowledge of cluster mass–observable scaling relations and other possible systematics are not expected to significantly degrade constraints [17]. The combination of clusters and voids will also help to minimize the impact of systematics. We leave the detailed impact of theoretical and observational systematics to be treated in future work.

E. Comparison to other probes

Current best limits on the sum of neutrino masses are $M_\nu < 0.10\text{--}0.15$ eV (95 % CL) assuming a flat Λ CDM cosmology [11, 33]. The stated range reflects different assumptions about the Hubble parameter and *Planck* cosmic microwave background (CMB) systematics. Cosmological data weakly favours a normal mass hierarchy, with the level of significance depending on assumptions about parameter priors [40]. Neutrino oscillation experiments provide stronger, though not yet decisive, evidence in favour of a normal hierarchy [33, 34, 41].

Cosmological data are likely to remain a very competitive, albeit model-dependent, probe of neutrino masses for the foreseeable future [41, 42]. The combination of CMB data from *Planck*, the proposed CORE or CMB-S4 missions, with future large-scale galaxy clustering, cosmic shear and intensity mapping surveys (e.g. *Euclid*, the Large Synoptic Survey Telescope, the Square Kilometer Array) are expected to reach $\sigma(M_\nu) \sim 15\text{--}25$ meV, $\sigma(w_0) \sim 0.002\text{--}0.008$ for minimal neutrino masses. For the (w_0, w_a) dark energy model, the expectations are $\sigma(M_\nu) \sim 15\text{--}30$ meV, $\sigma(w_0) \sim 0.002\text{--}0.02$, $\sigma(w_a) \sim 0.01\text{--}0.05$ [41, 43–45]. Since knowledge of the optical depth to reionization τ is a limiting factor for CMB neutrino mass constraints, the addition of a prior on τ from epoch of reionization (EoR) 21cm data can further reduce these uncertainties [46]. The 21cm power spectrum in the EoR (and earlier times) can also provide independent constraints on neutrino masses [41]. CMB-S4 cluster abundance also has great potential to provide strong constraints on dark energy and neutrino mass [43].

Cluster and void number densities as a function of characteristic size R_L scale as $n(R_L) \sim \exp(-\delta_c^2/\sigma_{R_L}^2)$, where δ_c is some characteristic linear density contrast threshold and $\sigma_{R_L}^2$ is the matter power spectrum smoothed on the scale R_L . Hence, cluster and void number counts are exponentially sensitive to the matter power spectrum on different scales. In contrast to CMB experiments, cluster - void samples have the advantages of probing the redshift evolution of expansion and structure growth directly, and not being degenerate with the optical depth to reionization.

Comparing the expected measurement precision from future experiments discussed above to Table I, large-area cluster and void cosmology with, e.g., *Euclid* can clearly be competitive with these experiments, in the best-case EV-B scenarios. The worst-case EV-A scenarios are not as competitive, though still provide informative independent constraints. These conclusions are robust if also accounting for cluster-void correlations (EC-LO).

V. CONCLUSION

Combining void and cluster counts could enable strong, simultaneous constraints on dark energy properties and neutrino properties, competitive with other future survey probes. Voids drive the neutrino mass constraint thanks to their wide range of sensitivity to the matter power spectrum across scales. Clusters add an orthogonal sensitivity to the mean matter density Ω_m that breaks degeneracy between expansion/growth and power spectrum to constrain both dark energy and neutrino mass.

Independent of other data and assuming minimal, normal-hierarchy neutrino masses, we forecast that *Euclid* joint cluster and void number counts could reach

$$\sigma(M_\nu) \lesssim 15 \text{ meV}, \quad (26)$$

$$\sigma(w_0) \lesssim 0.02, \quad (27)$$

$$\sigma(w_a) \lesssim 0.07, \quad (28)$$

$$B_{\text{NO,IO}} \gtrsim 130 : 1, \quad (29)$$

$$\text{FoM}(w_0, w_a) \gtrsim 4600, \quad (30)$$

if all information in void radius and density bins can be used (EV-B + EC-LO), or at worst

$$\sigma(M_\nu) \lesssim 52 \text{ meV},^2 \quad (31)$$

$$\sigma(w_0) \lesssim 0.03, \quad (32)$$

$$\sigma(w_a) \lesssim 0.12, \quad (33)$$

$$B_{\text{NO,IO}} \gtrsim 2.3 : 1, \quad (34)$$

$$\text{FoM}(w_0, w_a) \gtrsim 640, \quad (35)$$

if only the total number of deep voids above the survey limiting radius in redshift bins can be used (EV-A + EC-LO). Note however that the full cluster-only

² Corresponding to $M_\nu < 0.19$ eV ($\gtrsim 95\%$), taking $M_\nu \geq 0$ into account.

constraints (EC) on (w_0, w_a) are stronger than these [$\sigma(w_0) = 0.01, \sigma(w_a) = 0.04, \text{FoM}(w_0, w_a) = 3500$], since EC-LO includes only low-redshift ($z = 0.2 - 0.7$) clusters to account in a very conservative way for the potential degradation due to cluster-void correlations.

An inverted neutrino hierarchy could, in the best-case scenario, be rejected at the $\gtrsim 99\%$ level using Bayes factor model comparison (with uniform nonrestrictive parameter priors). In the worst-case scenario, it is not possible to statistically distinguish between the two neutrino mass hierarchies. These findings are robust with respect to cluster-void correlations and our alternative fiducial model (and thus robust to whether *Planck* 2015 or 2018 fiducial parameters are considered).

Since the combination of clusters and voids breaks parameter degeneracies in the histories of expansion and of structure growth, these conclusions are independent of whether dark energy has a constant, $w(z) = w_0$, or time-varying, $w(z) = w_0 + w_a z / (1 + z)$, equation of state. The most optimistic precision achievable with clusters and voids alone is $\sigma(M_\nu) \lesssim 11 \text{ meV}$, $\sigma(w_0) \lesssim 0.009$, $\sigma(w_a) \lesssim 0.03$.

Cluster and void cosmology with future large-area surveys such as *Euclid* has the potential to provide competitive constraints on extended cosmological models including massive

neutrinos or time-varying dark energy, in a way that is independent of the cosmic microwave background and the conventional probes in galaxy surveys (e.g. galaxy clustering, weak lensing / cosmic shear). The development of the theoretical aspects and of the data analysis methodology which will allow us to fully exploit the potential of cluster and void counts will be the subject of further studies.

VI. ACKNOWLEDGMENTS

Thanks are due to O. Botner, M. Gerbino, A. Hawken, A. Pisani, C. Reyes de los Heros, S. Riemer-Sørensen, R. Sheth, J. Silk and F. Villaescusa-Navarro for useful comments and conversations. I am grateful to the anonymous referee for very constructive feedback. The computations were performed on resources provided by SNIC through the Uppsala Multidisciplinary Center for Advanced Computational Science (UPPMAX) under Projects No. SNIC 2017/1-260 and No. SNIC 2018/3-283. M. S. was supported by Stiftelsen Olle Engkvist Byggmästare Project No. 2016/150.

-
- [1] S. W. Allen, A. E. Evrard, and A. B. Mantz, *Annu. Rev. Astron. Astrophys.* **49**, 409 (2011), 1103.4829.
 - [2] A. Pisani, P. M. Sutter, N. Hamaus, E. Alizadeh, R. Biswas, B. D. Wandelt, and C. M. Hirata, *Phys. Rev. D* **92**, 083531 (2015), 1503.07690.
 - [3] M. Sahlén, Í. Zubeldía, and J. Silk, *Astrophys. J. Lett.* **820**, L7 (2016), 1511.04075.
 - [4] T. Y. Lam, J. Clampitt, Y.-C. Cai, and B. Li, *Mon. Not. R. Astron. Soc.* **450**, 3319 (2015), 1408.5338.
 - [5] M. Sahlén and J. Silk, *Phys. Rev. D* **97**, 103504 (2018).
 - [6] J. Brandbyge, S. Hannestad, T. Haugbølle, and Y. Y. Y. Wong, *J. Cosmol. Astropart. Phys.* **9**, 014 (2010), 1004.4105.
 - [7] E. Massara, F. Villaescusa-Navarro, M. Viel, and P. M. Sutter, *J. Cosmol. Astropart. Phys.* **11**, 018 (2015), 1506.03088.
 - [8] S. Chongchitnan and J. Silk, *Astrophys. J.* **724**, 285 (2010), 1007.1230.
 - [9] A. Lewis, A. Challinor, and A. Lasenby, *Astrophys. J.* **538**, 473 (2000), astro-ph/9911177.
 - [10] E. V. Linder, *Phys. Rev. Lett.* **90**, 091301 (2003), astro-ph/0208512.
 - [11] Planck Collaboration, N. Aghanim, Y. Akrami, M. Ashdown, J. Aumont, C. Baccigalupi, M. Ballardini, A. J. Banday, R. B. Barreiro, N. Bartolo, et al., arXiv e-prints arXiv:1807.06209 (2018), 1807.06209.
 - [12] Planck Collaboration, P. A. R. Ade, N. Aghanim, M. Arnaud, M. Ashdown, J. Aumont, C. Baccigalupi, A. J. Banday, R. B. Barreiro, J. G. Bartlett, et al., *Astron. Astrophys.* **594**, A13 (2016), 1502.01589.
 - [13] C. Patrignani and Particle Data Group, *Chinese Physics C* **40**, 100001 (2016).
 - [14] G. Mangano, G. Miele, S. Pastor, T. Pinto, O. Pisanti, and P. D. Serpico, *Nuclear Physics B* **729**, 221 (2005), hep-ph/0506164.
 - [15] P. F. de Salas and S. Pastor, *J. Cosmol. Astropart. Phys.* **7**, 051 (2016), 1606.06986.
 - [16] R. Laureijs, J. Amiaux, S. Arduini, J. . Auguères, J. Brinchmann, R. Cole, M. Cropper, C. Dabin, L. Duvet, A. Ealet, et al., ArXiv e-prints (2011), 1110.3193.
 - [17] B. Sartoris, A. Biviano, C. Fedeli, J. G. Bartlett, S. Borgani, M. Costanzi, C. Giocoli, L. Moscardini, J. Weller, B. Ascaso, et al., *Mon. Not. R. Astron. Soc.* **459**, 1764 (2016), 1505.02165.
 - [18] A. Raccanelli, F. Montanari, D. Bertacca, O. Doré, and R. Durrer, *J. Cosmol. Astropart. Phys.* **5**, 009 (2016), 1505.06179.
 - [19] M. LoVerde, *Phys. Rev. D* **90**, 083530 (2014), 1405.4855.
 - [20] A. Banerjee and N. Dalal, *J. Cosmol. Astropart. Phys.* **11**, 015 (2016), 1606.06167.
 - [21] C. D. Kreisch, A. Pisani, C. Carbone, J. Liu, A. J. Hawken, E. Massara, D. N. Spergel, and B. D. Wandelt, arXiv e-prints arXiv:1808.07464 (2018), 1808.07464.
 - [22] M. Sahlén, P. T. P. Viana, A. R. Liddle, A. K. Romer, M. Davidson, M. Hosmer, E. Lloyd-Davies, K. Sabirli, C. A. Collins, P. E. Freeman, et al., *Mon. Not. R. Astron. Soc.* **397**, 577 (2009), 0802.4462.
 - [23] J. Lesgourgues, G. Mangano, G. Miele, and S. Pastor, *Neutrino Cosmology* (Cambridge University Press, Cambridge, UK, 2013).
 - [24] G. R. Blumenthal, L. N. da Costa, D. S. Goldwirth, M. Lecar, and T. Piran, *Astrophys. J.* **388**, 234 (1992).
 - [25] E. Jennings, Y. Li, and W. Hu, *Mon. Not. R. Astron. Soc.* **434**, 2167 (2013), 1304.6087.
 - [26] F. Bernardeau, *Astrophys. J.* **427**, 51 (1994), astro-ph/9311066.
 - [27] T. Ronconi and F. Marulli, *Astron. Astrophys.* **607**, A24 (2017), 1703.07848.
 - [28] P. S. Corasaniti and I. Achitouv, *Phys. Rev. Lett.* **106**, 241302 (2011), 1012.3468.
 - [29] R. Voivodic, M. Lima, C. Llinares, and D. F. Mota, *Phys. Rev. D* **95**, 024018 (2017), 1609.02544.
 - [30] P. T. P. Viana and A. R. Liddle, *Mon. Not. R. Astron. Soc.* **281**, 323 (1996), astro-ph/9511007.

- [31] X. Qian, A. Tan, W. Wang, J. J. Ling, R. D. McKeown, and C. Zhang, *Phys. Rev. D* **86**, 113011 (2012), 1210.3651.
- [32] M. Blennow, *J. High Energy Phys.* **1**, 139 (2014), 1311.3183.
- [33] S. Vagnozzi, E. Giusarma, O. Mena, K. Freese, M. Gerbino, S. Ho, and M. Lattanzi, *Phys. Rev. D* **96**, 123503 (2017), 1701.08172.
- [34] P. F. de Salas, D. V. Forero, C. A. Ternes, M. Tortola, and J. W. F. Valle, *Phys. Lett.* **B782**, 633 (2018), 1708.01186.
- [35] K. Olive and P. D. Group, *Chinese Physics C* **38**, 090001 (2014), URL <http://stacks.iop.org/1674-1137/38/i=9/a=090001>.
- [36] H. Jeffreys, *The Theory of Probability* (Oxford University Press, Oxford, UK, 1939).
- [37] G. Pollina, N. Hamaus, K. Dolag, J. Weller, M. Baldi, and L. Moscardini, *Mon. Not. R. Astron. Soc.* **469**, 787 (2017), 1610.06176.
- [38] G. Pollina, N. Hamaus, K. Paech, K. Dolag, J. Weller, C. Sánchez, E. S. Rykoff, B. Jain, T. M. C. Abbott, S. Allam, et al., *ArXiv e-prints* (2018), 1806.06860.
- [39] N. Hamaus, A. Pisani, P. M. Sutter, G. Lavaux, S. Escoffier, B. D. Wandelt, and J. Weller, *Phys. Rev. Lett.* **117**, 091302 (2016), 1602.01784.
- [40] S. Gariazzo, M. Archidiacono, P. F. de Salas, O. Mena, C. A. Ternes, and M. Tórtola, *J. Cosmol. Astropart. Phys.* **3**, 011 (2018), 1801.04946.
- [41] P. F. de Salas, S. Gariazzo, O. Mena, C. A. Ternes, and M. Tórtola, *Frontiers in Astronomy and Space Sciences* **5**, 36 (2018), 1806.11051.
- [42] R. B. Patterson, *Annual Review of Nuclear and Particle Science* **65**, 150807173859001 (2015).
- [43] K. N. Abazajian, P. Adshead, Z. Ahmed, S. W. Allen, D. Alonso, K. S. Arnold, C. Baccigalupi, J. G. Bartlett, N. Battaglia, B. A. Benson, et al., *ArXiv e-prints* (2016), 1610.02743.
- [44] R. Ruggeri, E. Castorina, C. Carbone, and E. Sefusatti, *J. Cosmol. Astropart. Phys.* **3**, 003 (2018), 1712.02334.
- [45] T. Sprenger, M. Archidiacono, T. Brinckmann, S. Clesse, and J. Lesgourgues, *ArXiv e-prints* (2018), 1801.08331.
- [46] M. Archidiacono, T. Brinckmann, J. Lesgourgues, and V. Poulin, *J. Cosmol. Astropart. Phys.* **2**, 052 (2017), 1610.09852.